Korean J. Chem. Eng., 40(9), 2321-2333 (2023)
DOI: 10.1007/s11814-023-1442-y

pISSN: 0256-1115
eISSN: 1975-7220

Visibly transparent UV protection and adjusted mechanical properties of films composed of lignin-derived wastes and poly[(R)-3-hydroxybutyric acid]

Aliaksandr Karnitski[*,], Jae-Wook Choi[*], Heesuk Kim[**,***], Chun-Jae Yoo[*], Hyunjoo Lee[*,**], Dong Jin Suh[*], Kwang Ho Kim[*,**], Changsoo Kim[*,**], Kyeongsu Kim[*,**], and Jeong-Myeong Ha[*,**,†]**

*Clean Energy Research Center, Korea Institute of Science and Technology, Seoul 02792, Korea
**Division of Energy and Environment Technology, KIST School, University of Science and Technology, Seoul 02792, Korea
***Soft Hybrid Materials Research Center, Korea Institute of Science and Technology, Seoul 02792, Korea
(*Received 11 November 2022 • Revised 3 January 2023 • Accepted 31 January 2023*)

Abstract−Blended films composed of poly[(R)-3-hydroxybutyric acid] (P3HB) and lignin wastes were prepared to adjust the mechanical and optical properties of P3HB films. In addition to the organosolv lignin extracted from oak, the oligomeric or polymeric byproducts obtained during the reductive catalytic depolymerization of lignin were mixed with P3HB. This adjusted the mechanical and optical properties of films to manipulate biodegradable P3HB films and create new applications of lignin wastes. When the solid residue obtained from depolymerization of organosolv lignin in an aqueous methanol solution was mixed with P3HB, the elongation at the break increased from 1.6±0.3% to 4.9±1.0% and Young's modulus decreased from 1.97±0.21 GPa to 0.98±0.11 GPa depending on the depolymerization conditions. The films composed of P3HB and organosolv lignin blocked UV and a great deal of visible light, exhibiting 0.3-11.1% transmittance of UVA and 24.8-61.6% transmittance of visible light. However, those composed of P3HB and depolymerized lignin prepared during lignin depolymerization exhibited significant UV blocking with good transparency, featuring 0.7-39.8% transmittance of UVA and 33.7-78.3% transmittance of visible light. The adjusted mechanical and optical properties of blended films can be attributed to the interaction between P3HB and lignin derivatives. This study can be useful to valorize lignin-based waste obtained during the process of depolymerizing lignin to valuable phenolic monomers. Moreover, it can contribute to the development of the lignin-based sustainable chemical industry.

Keywords: Poly[(R)-3-hydroxybutyric Acid], Lignin, Film, Solvent Casting, Lignin Depolymerization

INTRODUCTION

The production of sustainable materials using renewable feedstock as a fossil fuel substitute is key to achieving a carbon-neutral industry. Among the carbon-based materials prepared from fossil fuels, plastics for packaging have been mass-produced, and their substitution with a corresponding sustainable polymer can significantly reduce the discharge of plastic wastes and the consumption of fossil fuels, thereby improving carbon-neutral growth.

Plastic packaging materials are made of polymer films, including polyethylene (PE), polypropylene (PP), and polyethylene terephthalate (PET), which contribute to climate change and environmental pollution because they are prepared from fossil fuels and their natural degradation is extremely difficult. Biodegradable polymers have been prepared using natural sources to replace current conventional plastics. Polyhydroxyalkanoates (PHAs) are frequently suggested biodegradable plastics that can be biologically prepared [1]. Polyhydroxybutyrate is a commonly used PHA produced from glucose through a biological process. Poly-3-hydrobutyrate (P3HB), poly-4-hydrobutyrate (P4HB), polyhydroxyvalerate (PHV), and their copolymers have been used for manufacturing films [2-4]. Mass production of PHAs has been achieved, but the application of these polymers is limited because of their poor mechanical properties.

To improve the properties of these PHAs for commercial use and replace current conventional polymer products, polymer blends composed of several polymers were prepared [2,5-9] (Table 1). To maintain the biodegradability of PHAs, lignin, as a natural polymer, was mixed with PHAs [5,10], and the mechanical and optical properties were adjusted. Polybutylene adipate-co-terephthalate (PBAT) and polylactic acid (PLA) blended with lignin were also prepared to achieve biodegradable films exhibiting improved mechanical and thermal properties [6,7,11]. In addition to such enhanced thermal and mechanical properties, lignin-containing composites can be used as transparent UV blocking films [12-14].

Valorizing lignin, a byproduct of lignocellulose to sugars, has been attempted because it is used as low-quality solid fuel. Previous studies investigated the depolymerization of lignin to obtain phenolic monomers that can replace current petroleum-based feedstock in the chemical industry [15-17]. While phenolic monomers can be obtained from lignin, their harsh reaction conditions and low yields produce byproducts such as oligomers, polymers, and char. Although these byproducts cannot be easily valorized, they can be mixed with other materials to manipulate their properties; similarly, lignin has also been mixed with conventional polymer to improve its mechanical properties [8,9]. By valorizing these oligomers and polymers derived from lignin, a wide use of lignin can be achieved,

†To whom correspondence should be addressed.
E-mail: jmha@kist.re.kr
Copyright by The Korean Institute of Chemical Engineers.

Table 1. Literature data related to mechanical properties of lignin-added polymer blend films

Lignin	Lignin content (%)	Polymer	Preparation method	Film size (mm)	Strain rate (mm/min)	Tensile strength (MPa)	Elongation at break (%)	Young's modulus (MPa)	Reference
"Lignocreosol" lignin	0	PHB[a]	Chloroform solution casting	33×6 with 1-1.5 mm thickness	10	8.3	310		[2]
	3					9.9	320		
	6					9.2	50		
	9					8.8	40		
	12					8.7	5		
Kraft lignin	0	P3HB[b]	Hot press	50	10	18.8	5.7	990	[5]
	5					21.2	5.2	1,240	
	7					21.3	4	1,410	
	9					21.1	3.1	1,440	
OL from grape seeds	0	PHB[a]-PHA[c] (1 : 1)	Chloroform solution casting	20×0.15	1	6.6	95.2	240	[6]
	1					29	68	302	
	5					36	82	200	
	10					13	15	827	
Alkaline soda lignin	0	PBAT[d]	Hot press	0.060-0.090		29	655	46	[7]
	10					25	418	63	
	20					14	322	62	
Alkaline soda lignin esterified using 10-undecenoyl chloride	10	PBAT[d]	Hot press	0.060-0.090		29	689	34	[7]
	20					26	632	37	
Alkaline soda lignin esterified (oleoyl chloride)	10	PBAT[d]	Hot press	0.060-0.090		30	679	20	[7]
	20					21	522	23	
Kraft lignin (pine)	0	LLDPE[e]	Melt extrusion	50×0.045	50	14.06	357.41	323	[8]
	2.5					9.75	339.22	369	
	5					9.45	348.35	353	
	10					7.51	290.25	343	
Esterified Kraft lignin (eucalyptus)	2.5	LLDPE[e]	Melt extrusion	50×0.045	50	9.42	351.33	221	[8]
	5					8.69	212	226	
	10					7.31	242.98	193	
Björkman lignin	0	PE[f]	*m*-Xylene solution casting	25×0.15	1	18.4	752	351	[9]
	2					18	753	395	

[a]PHB: polyhydroxybutyrate. [b]P3HB: poly(3-hydroxybutyrate). [c]PHA: polyhydroxyalkanoate. [d]PBAT: polybutylene adipate terephthalate. [e]LLDPE: linear low density polyethylene. [f]PE: polyethylene

and current petroleum feedstock can be replaced with biomass resources for a more sustainable industry.

In this study, poly[(R)-3-hydrobxybutyric acid] (P3HB) was mixed with organosolv lignin (OL) extracted from oak and its derivatives for preparing biodegradable films. We attempted to modify the optical, thermal, and mechanical properties for preparing biodegradable functional polymer films by adding OL to P3HB. Compared to previous studies [2,5-9], we used the byproducts obtained during the depolymerization of lignin to phenolic monomers (Scheme 1). During lignin depolymerization, i.e., the reductive catalytic depolymerization proposed in this study, solid residue (SR) and depolymerized lignin oligomer (DL) were obtained as byproducts, which are less valuable compared to phenolic monomers. In this study, these byproducts were used as additives of biodegradable P3HB films, thereby exploiting the whole lignin reactant. The byproducts can also contribute to improving the economic feasibility of the lignin valorization process. This strategy of valorizing the whole lignin reactant can contribute to building a biomass-based society.

MATERIALS AND METHODS

1. Materials

Organosolv lignin (OL) extracted from oak was purchased from Sugaren (Yongin, Korea). Poly[(R)-3-hydroxybutyrate] (P3HB), chloroform (99.9%), pyridine (anhydrous, 99.8%), acetic anhydride (99%), ethanol (anhydrous, 99.5%), chromium (III) acetylacetonate ($Cr(C_5H_7O_2)_3$, 99.9%), deuterated chloroform ($CDCl_3$, 99.96%), and cyclohexanol (99%) were purchased from Sigma Aldrich (Milwaukee, Wisconsin, USA). 2-Chloro-4,4,5,5-tetramethyl-1,3,2-dioxaphospholane (TMDP, 95%) was purchased from Chem Cruz (Dallas,

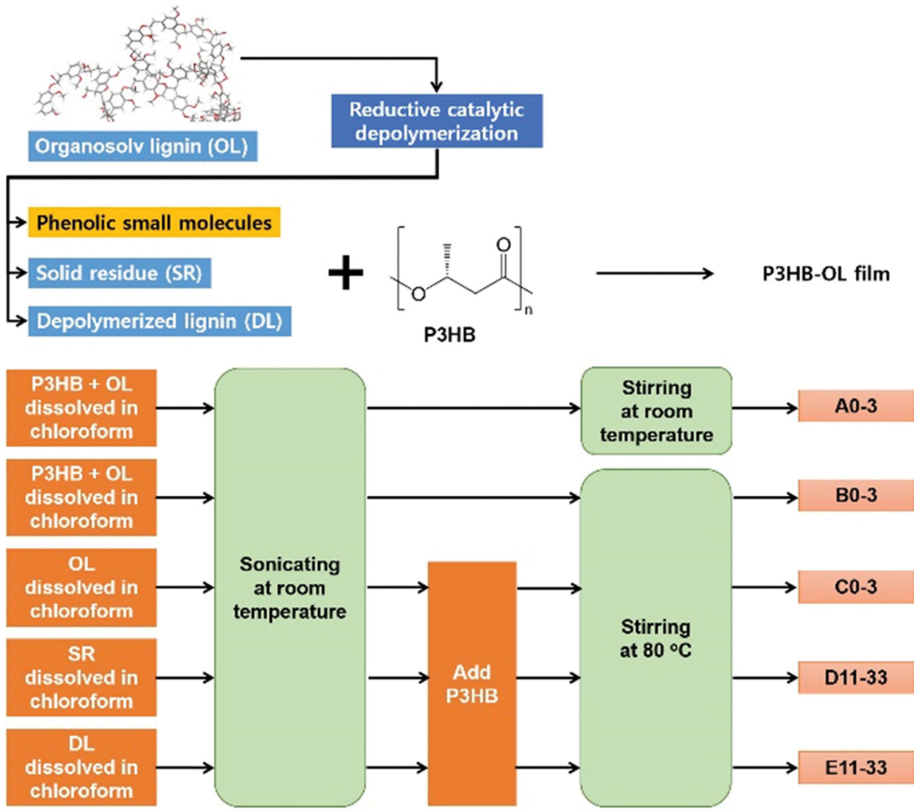

Scheme 1. Preparation of OL-PHB blended films.

Texas, USA), sulfuric acid (aqueous, 72%) was purchased from J.T. Baker (Phillipsburg, New Jersey, USA), and tetrahydrofuran (THF) was purchased from Honeywell B&J (Morris Plains, New Jersey, USA). Deionized water (DI water) was prepared using an Arium comfort I Bench-Top water purification system (Sartorius; Göttingen, Germany).

2. Compositional Analysis and Gel Permeation Chromatography of Lignin

The weight fraction of lignin was measured using a method reported in the literature [18,19]. A two-step hydrolysis process was performed. The lignin sample (0.5 g, dry) was treated with a 72% aqueous sulfuric acid solution at 30 °C for 1 h in a water bath. The mixture was diluted to 4% sulfuric acid using 84 mL of deionized water (18.2 MΩ·cm), heated to 121 °C for 2 h, and then slowly cooled to room temperature. The remaining residue was separated by filtration, dried, and weighed, representing the weight of the acid-insoluble lignin. All processes were performed using pressure tubes (8648-30 ACE glass) and screw-on Teflon caps with O-ring seals. Thermal stability was measured using a Q500 thermogravimeter (TA Instruments; New Castle, Delaware, USA). The samples (approximately 10 mg) were heated to 105 °C to remove the moisture and then heated to 600 °C. The measurements were performed in air atmosphere (flow rate of 30 mL/min, heating rate of 10 °C/min). Gel permeation chromatography (GPC) was used to obtain the molecular weight distributions of the polymer mixture and measure the number-average molecular weight (M_n), weight-average molecular weight (M_w), and polydispersity index (PDI=M_w/M_n) [17,20,21]. Agilent 1200 HPLC equipped with two Shodex LF-804 columns and a UV detector (270 nm) was used with a tetrahydrofuran eluent (flow rate: 1.00 mL/min). The column was calibrated using a simulated polystyrene standard ReadyCal set (Sigma-Aldrich, 250-2,000,000 g/mol). Acetylated lignin was dissolved in THF at a concentration of 1 g/L and filtered using a 0.45-mm Whatman syringe filter prior to injection into the GPC system. ^{31}P NMR measurements of lignin reactant and lignin residues were performed at the KIST Advanced Analysis Center (Seoul, Korea) using a 400-MHz Agilent spectrometer with an inverse gated proton decoupling pulse. The samples were prepared and characterized according to methods described in the literature [21-26]. Lignin (approximately 30 mg) samples were dissolved in a mixture of pyridine and $CDCl_3$ (pyridine : $CDCl_3$=1 : 1 by weight), and an internal standard (cyclohexanol) and relaxation agent (chromium(III) acetylacetonate) dissolved in $CDCl_3$ were added to the mixture. TMDP was added, and the sample was transferred into an NMR tube for ^{31}P NMR analysis.

3. Film Preparation

Films composed of P3HB and OL were prepared by casting a chloroform-dissolved solution on a Petri dish (Scheme 1). OL dissolved in chloroform was sonicated to improve the dispersion of lignin powder. Depending on the film preparation methods, mixtures containing P3HB and OL were stirred at room temperature or at 80 °C in an oil bath for 1 h before transferring to a Petri dish. The polymer mixture concentrations in chloroform were fixed to 20 g/L. The prepared films were dried under ambient conditions

before characterization. In addition to OL, the lignin derivatives obtained during the reductive catalytic depolymerization of OL were also mixed with P3HB, as reported in a previous study of ours [16]. While an aqueous methanol was used in that previous study [16], 50, 75, and 100% aqueous methanol solvents were used in the present one. The reductive depolymerization reaction of lignin was performed at 280 °C for 6 h with ruthenium supported on Hβ zeolite (metal content of 3 wt%). The mixture, composed of 2 g of OL and 0.2 g of catalyst dispersed in 30 mL of solvent, was used for the reaction. The DL, dissolved in the solvent, and SR, not dissolved in the solvent, were separated by centrifugation, following solvent removal under vacuum drying for 16 h. The solid residues (SRs) prepared in 50, 75, and 100% aqueous methanol solvents are denoted as SR50, SR75, and SR100, respectively. Similarly, the depolymerized lignins (DLs) prepared in 50, 75, and 100% aqueous methanol solvents are denoted as DL50, DL75, and DL100, respectively. SRs and DLs replaced OL when they were used for preparing blended films.

4. Characterization of OL-P3HB Blends

Thermodynamic properties of polymer blends were observed using differential scanning calorimetry (DSC). The glass transition temperature (T_g, at the heating step), freezing temperature (T_f, at the cooling step), crystallization temperature (T_c, at the heating step), and melting temperature (T_m, at the heating step) of the polymer were determined while the polymer samples were heated from −10 to 200 °C, isothermally held at 200 °C for 1 min, and cooled back to −10 °C. The measurements were cycled several times. The thermal properties of polymer blends were observed using thermogravimetry (TG). The measurements were performed in nitrogen (N_2) flow (30 mL/min). The sample (approximately 10 mg) was heated from room temperature to 100 °C at a heating rate of 10 °C/min, isothermally kept at 100 °C for 30 min, and heated to 800 °C at a heating rate of 10 °C/min. The mechanical properties were measured using a Cometech QC-508E universal testing machine (Cometech; Taichung City, Taiwan). All measurements were performed using 40×10 mm^2 films at room temperature (24-27 °C) under ambient conditions. The films were stretched to failure at 1 mm/min. Scanning electron microscopy (SEM) images of films were obtained using Inspect F50 (ThermoFisher; Waltham, Massachusetts, USA). The device was operated in high-vacuum mode at an acceleration voltage of 3 kV. The samples for cross-section measurements were held in liquid N_2 for approximately 3 min prior to platinum coating. The optical properties of films were measured using a Cary 500 dual beam ultraviolet-visible (UV-Vis NIR; Agilent; Santa Clara, California, USA). The transmittance was measured in the range of 200-800 nm. The average UVA, UVB, and UV protection factors of films were calculated using a standard AS/NZS4399.

RESULTS AND DISCUSSION

1. Thermodynamic Properties and Crystal Structures of P3HB-OL blend

The compositional analysis of organosolv oak lignin indicated that the fraction of acid-insoluble lignin was 91.8±0.9 wt% with 2.4±0.6 wt% moisture and 2.6±0.6 wt% ash. The moisture was removed by holding the lignin reactant at 105 °C for 2 h prior to use. Before preparing P3HB-OL blended films, the thermodynamic

Table 2. Thermal properties of P3HB-OL blends

	Polymer	100% OL	100% P3HB	95% P3HB, 5% OL	90% P3HB, 10% OL	80% P3HB, 20% OL
1st run	T_g (°C)	n.a.	n.a.	n.a.	n.a.	n.a.
	ΔH_c (J/g P3HB) at T_c (°C)[b]	n.a.	n.a.	n.a.	n.a.	n.a.
	ΔH_m (J/g P3HB) at T_m (°C)	n.a.	92.1 at 176.0	91.2 at 175.2	92.2 at 175.2	93.9 at 175.0
	ΔH_f (J/g P3HB) at T_f (°C)	n.a.	71.9 at 89.0	62.1 at 71.9	54.6 at 70.9	42.0 at 68.7
	$\Delta H_c/\Delta H_m$	n.a.	0.0	0.0	0.0	0.0
2nd run	T_g (°C)	n.a.	n.a.	n.a.	4.4	5.1
	ΔH_c (J/g P3HB) at T_c (°C)[b]	n.a.	7.9 at 66.5	14.1 at 50.0	23.2 at 51.2	40.3 at 51.4
	ΔH_m (J/g P3HB) at T_m (°C)	n.a.	92.7 at 172.4	90.7 at 172.0, 174.8	91.2 at 172.6, 174.4	92.5 at 171.6, 174.5
	ΔH_f (J/g P3HB) at T_f (°C)	n.a.	74.4 at 84.1	60.2 at 71.6	39.0 at 63.1	20.0 at 64.3
	$\Delta H_c/\Delta H_m$	n.a.	0.085	0.155	0.255	0.435
3rd run	T_g (°C)	n.a.	n.a.	n.a.	4.2	4.0
	ΔH_c (J/g P3HB) at T_c (°C)[b]	n.a.	7.5 at 65.8	17.4 at 49.7	41.3 at 51.2	67.3 at 52.3
	ΔH_m (J/g P3HB) at T_m (°C)	n.a.	93.0 at 170.3	90.7 at 170.2, 174.8	90.1 at 169.1, 174.9	91.6 at 174.3
	ΔH_f (J/g P3HB) at T_f (°C)	n.a.	77.2 at 84.0	59.9 at 69.4	36.6 at 62.2	20.6 at 65.8
	$\Delta H_c/\Delta H_m$	n.a.	0.081	0.191	0.459	0.734
4th run	T_g (°C)	n.a.	n.a.	n.a	4.1	4.0
	ΔH_c (J/g P3HB) at T_c (°C)[b]	n.a.	7.6 at 66.8	17.9 at 50.4	44.3 at 51.1	65.8 at 52.5
	ΔH_m (J/g P3HB) at T_m (°C)	n.a.	93.6 at 168.5, 174.7	90.7 at 167.9, 174.1	90.7 at 168.6, 174.3	91.8 at 166.3, 173.6
	ΔH_f (J/g P3HB) at T_f (°C)	n.a.	77.2 at 83.8	53.1 at 68.2	37.0 at 65.4	17.0 at 62.3
	$\Delta H_c/\Delta H_m$	n.a.	0.081	0.197	0.489	0.717

[a]All enthalpies were depicted based on the mass of P3HB fraction. [b]T_c, T_m, and T_f were measured at their peaks. [c]A broad peak was observed.

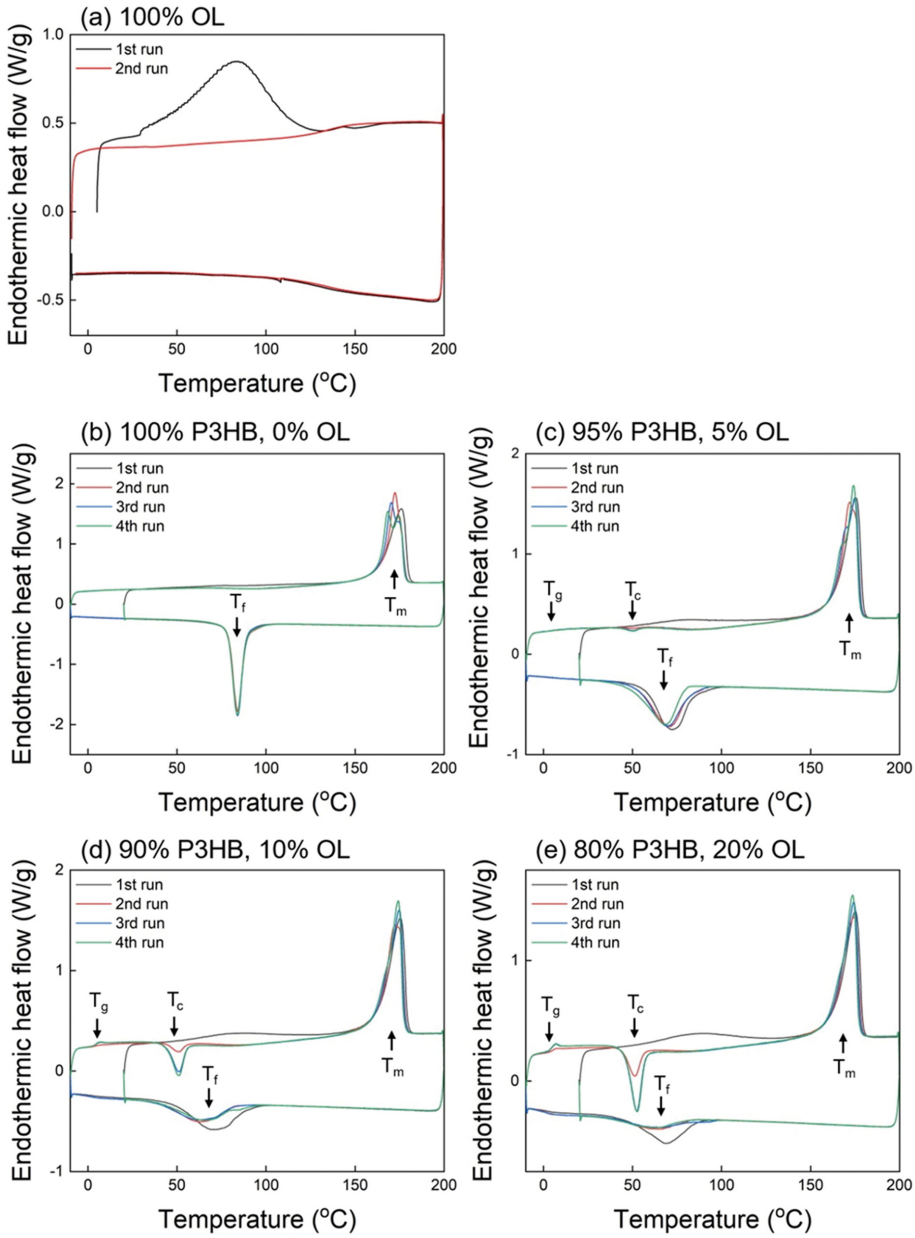

Fig. 1. DSC results of P3HB-OL mixtures.

properties of the P3HB-OL blend were observed using DSC (Table 2 and Fig. 1), which demonstrated that the crystallization of P3HB is suppressed by adding OL. The thermodynamic properties of P3HB and OL, without mixing, were observed (Table 2 and Fig. 1(a), (b)). Notably, the DSC measurements were performed up to 200 °C, while 1.0 wt% loss up to 100 °C and 2.4 wt% loss up to 200 °C were observed by the TG measurement of OL under N_2 environment. OL exhibited a broad endothermic peak at 25-135 °C with 117.1 J/g of enthalpy change. Because the solid phase of OL was not transformed to the other phase during heating and the TG measurement did not exhibit any significant loss indicating no evaporation of volatile compounds at this temperature range (Fig. S1), the endothermic peak is likely attributed to the collapse of the initial OL morphology. After the first cycle of heating to 200 °C and cooling to −10 °C, freezing with the exothermic peak was not observed. From the second cycle, no peaks of phase transition were observed at −10-200 °C. The P3HB powder, received from the commercial vendor, was heated and then cooled between −10 and 200 °C four times (Fig. 1(b)). For the first run of as-received P3HB powder, a melting peak at 176.0 °C with 87.8 J/g of melting enthalpy was observed. The P3HB melt was frozen at 84.0 °C while cooling, exhibiting 67.2 J/g of freezing enthalpy, indicating that 23% of P3HB melt was not frozen and formed an amorphous supercooled melt during the cooling step. For the second run, a melting peak was observed at 172.4 °C with 86.2 J/g of melting enthalpy. For the third and fourth runs, doublets of the melting peak were observed and the peak at the lower temperature became larger at the fourth run compared to the third run (Fig. 1(b)). The crystallization of

supercooled P3HB melt during the heating steps was observed at 7.5-7.9 °C with 65.8-66.8 J/g P3HB enthalpy for the second to fourth runs.

The mixtures of P3HB and OL were heated to 200 °C and cooled to −10 °C four times. The corresponding peaks for OL (Fig. 1(a)) and P3HB (Fig. 1(b)) were observed: endothermic peaks at 160-180 °C for the melting of P3HB, exothermic peaks at 40-100 °C (freezing temperature, T_f) for the freezing of P3HB, and endothermic peaks at 40-130 °C for the phase transition of OL. In addition to the peaks observed for each P3HB and OL, additional peaks formed during heating: glass transition at 4.1-5.1 °C (glass transition temperature, T_g) and crystallization at 40-60 °C (crystallization temperature, T_c). The presence of a glass transition in the P3HB and OL mixture can be attributed to their interaction; pure P3HB and OL did not exhibit a glass transition in this study. The melting temperatures (T_m) and melting enthalpies (ΔH_m) did not significantly change in presence of OL. The crystallization of P3HB during cooling from 200 °C was inhibited by the presence of OL, and the enthalpy of freezing during the cooling step decreased from 77.2 J/g P3HB to 53.1 (5% OL), 37.0 (10% OL), and 17.0 J/g P3HB (20% OL) compared to that of pure P3HB for the fourth run, indicating that larger concentrations of OL led to increased quantities of supercooled P3HB melt. The P3HB melt crystallized at 49.7-52.5 °C during the heating steps for 5-20% OL, which are lower temperatures than those observed for pure P3HB (65.8-66.8 °C). Notably, adding OL to P3HB can decrease the crystallization temperature (T_c) and increase the fraction of supercooled P3HB melt (Table 2). The decreased crystallinity of P3HB was also confirmed using XRD (Fig. S2). Representatively, the full width at half maximum (FWHM) of α(020) peak at 2θ=13.3° increased from 0.157° (P3HB) to 0.179° (after the fourth DSC cycle for 10% OL in OL-P3HB blend). The diffraction peak of the β-phase at 2θ=20.1° also became weaker and less clear with repeated melting and freezing cycles [27,28]. The FWHMs of diffractions at 2θ=20.1°, 21.4°, and 22.5° increased from 0.934°, 0.671°, and 0.886° (for P3HB), respectively, to 1.35°, 0.945°, and 1.05° (after the fourth DSC cycle for 10% OL in OL-P3HB blend), respectively, indicating less crystallinity.

2. Mechanical Properties of P3HB-OL Blended Films

Given that the P3HB-OL blended films prepared by the hot press method were not uniform in our lab (they exhibited formation of segregated dark particles (Fig. S3)), the films prepared by the solvent casting method were studied (Table 3 and Fig. 2). Prior to preparing the blended films, a method for preparing P3HB films without adding OL was determined based on their mechanical properties and the severity of the preparing conditions. As reported in the literature [2,6], the sonication of P3HB powder in chloroform at room temperature (entries A0 and B0) and the reflux conditions for P3HB-chloroform solutions (entries B0 and C0) were selected as preparation conditions for improving the dissolution of P3HB in chloroform (Scheme 1) and obtaining the uniform films. Concerning the P3HB film without adding OL, the refluxing condition (entry B0) increased the tensile strength, 29.6±3.6 MPa (entry B0) compared to 19.4±2.9 MPa (no reflux, entry A0), and Young's modulus, 1.98±0.19 GPa (entry B0) compared to 1.60±0.19 GPa (no reflux, entry A0). The elongation at break slightly increased for the reflux condition (1.6±0.2% and 2.0±0.5% for entries A0 and B0, respectively). When only OL, not P3HB, was sonicated, the tensile strength slightly decreased to 27.0±3.7 MPa and Young's modulus increased to 1.97±0.21 GPa (entry C0 compared to entry A0). The elongation at the break was almost the same for entries A0 and C0. Although the sonication of P3HB powder may improve the dissolution of P3HB in chloroform, it can mechanically degrade the structure of P3HB film; thus, we selected the

Table 3. Mechanical properties of prepared films composed of P3HB and OL[a,b]

Film	Entry	Lignin content (wt%)	Tensile strength (MPa, at maximum load)	Elongation at break (%)	Young's modulus (GPa)	Thickness (μm)
P3HB film (sonicating P3HB at room temperature, then stirring at room temperature)	A0	0	19.4±2.9	1.6±0.2	1.60±0.19	35±2
P3HB film (sonicating P3HB at room temperature, then stirring at 80 °C)	B0	0	29.6±3.6	2.0±0.5	1.98±0.19	26±1
P3HB film (stirring at 80 °C)	C0	0	27.0±3.7	1.6±0.3	1.97±0.21	31±2
OL-P3HB blended film (sonicating a mixture of OL and P3HB at room temperature, then stirring at room temperature)	A1	5	22.4±3.9	1.8±0.5	1.54±0.22	36±1
	A2	10	24.9±3.3	1.5±0.2	1.87±0.22	34±4
	A3	20	21.4±1.9	1.4±0.4	1.89±0.28	33±1
OL-P3HB blended film (sonicating a mixture of OL and P3HB at room temperature, then stirring at 80 °C)	B1	5	29.3±3.4	1.9±0.5	2.00±0.22	29±2
	B2	10	24.4±2.7	1.8±0.4	1.73±0.20	30±2
	B3	20	20.9±2.3	1.4±0.2	1.74±0.18	31±3
OL-P3HB blended film (sonicating OL at room temperature, then stirring of a mixture of OL and P3HB at 80 °C)	C1	5	28.1±3.6	1.6±0.3	2.01±0.25	31±3
	C2	10	22.3±1.9	1.2±0.2	1.99±0.26	31±2
	C3	20	18.0±2.8	1.3±0.3	1.78±0.23	35±2

[a]Preparation method depicted in Scheme 1. [b]Standard deviations calculated based on the measurements of 5-7 specimens.

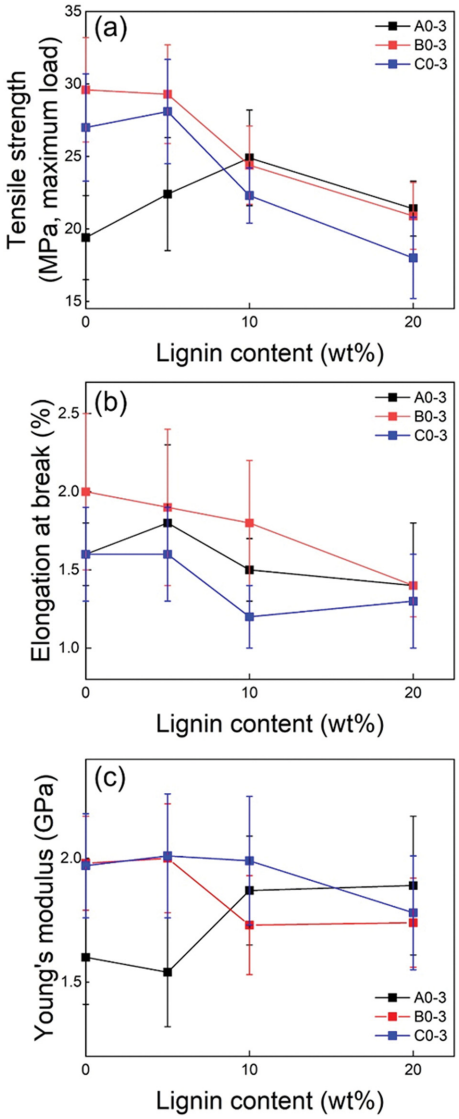

Fig. 2. Mechanical properties of P3HB-OL blended films.

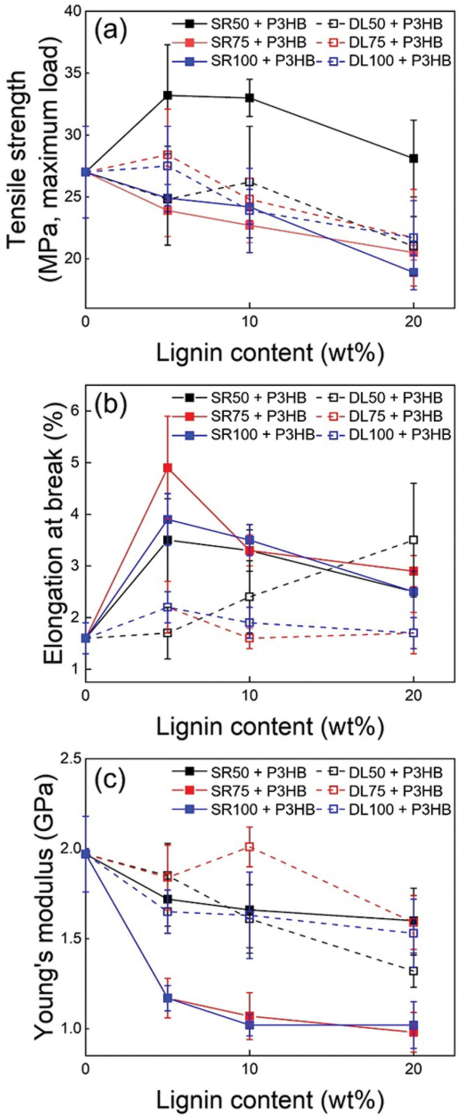

Fig. 3. Mechanical properties of P3HB-lignin derivative blended films.

reflux conditions for chloroform solution (entry C0) without the sonication of P3HB in chloroform to understand the effects of OL addition on the properties of P3HB-containing films. Notably, the stirring temperature selected in this study (80 °C) is lower than the melting temperature of P3HB (Fig. 1) and does not thermally degrade P3HB and OL (Fig. S1).

The effect of OL content was also measured for three different methods (entries A0, B0, and C0; Table 3 and Fig. 2). By increasing OL content, a decreasing tensile strength, a decreasing elongation at break, and a decreasing Young's modulus (except entry A1) were observed for all films prepared by entries A1-3, B1-3, and C1-3. For the method selected in this study (entries C1-3), the measured tensile strength decreased from 28.1±3.6 to 18.0±2.8 MPa with increasing OL content from 5 to 20 wt%. Young's moduli observed for OL-P3HB films were 1.2-1.6 GPa, lower than those of other films. The elongation at break also slightly decreased from 1.6±0.3 to 1.2±0.2 and 1.3-0.3% with increasing OL content from 5 to 20 wt%, respectively.

3. Mechanical Properties of SR- and DL-added P3HB Films

While OL was mixed with P3HB for preparing blended films, the byproducts of lignin depolymerization, including depolymerized lignin (DL) and solid residue (SR) prepared as reported in a previous study of ours [16], were also mixed with P3HB. Given that the applications of these oligomers, not fully depolymerized to phenolic monomers, are limited, the use of these byproducts as additives for functional materials can improve the feasibility of the lignin depolymerization process. When the blended films were prepared as depicted in Scheme 1, the mechanical properties of these films, prepared using the method of entries C0-3, were measured (Table 4). Compared to the P3HB film (entry C0), the addition of OL, SR, and DL slightly decreased the tensile strength, although the highest tensile strength was observed for the 5-10 wt% SR50-added P3HB film (33.0-33.2 MPa vs. 27.0 MPa for P3HB film). The elongations at break for SR- and DL-added films were larger than that of P3HB films; however, the elongations at break of OL-added

Table 4. Mechanical properties of prepared films composed of P3HB and lignin derivatives[a,b]

Film	Entry	Lignin derivative content (%)	Tensile strength (MPa, maximum load)	Elongation at break (%)	Young's modulus (GPa)	Thickness (μm)
P3HB	C0	0	27.0±3.7	1.6±0.3	1.97±0.21	31±2
OL+P3HB	C1	5	28.1±3.6	1.6±0.3	2.01±0.25	31±3
	C2	10	22.3±1.9	1.2±0.2	1.99±0.26	31±2
	C3	20	18.0±2.8	1.3±0.3	1.78±0.23	35±2
SR100+P3HB	D31	5	24.9±1.1	3.9±0.5	1.17±0.07	31±1
	D32	10	24.2±1.4	3.5±0.3	1.02±0.06	32±3
	D33	20	18.9±1.4	2.5±0.4	1.02±0.13	31±4
SR75+P3HB	D21	5	23.9±2.1	4.9±1.0	1.17±0.11	36±1
	D22	10	22.7±1.4	3.3±0.3	1.07±0.13	35±2
	D23	20	20.5±0.6	2.9±0.3	0.98±0.11	37±2
SR50+P3HB	D11	5	33.2±4.1	3.5±0.8	1.72±0.15	26±1
	D12	10	33.0±1.5	3.3±0.4	1.66±0.21	27±2
	D13	20	28.1±3.1	2.5±0.4	1.60±0.18	28±3
DL100+P3HB	E31	5	27.5±3.2	2.2±0.3	1.65±0.12	33±3
	E32	10	23.9±3.4	1.9±0.3	1.63±0.24	29±1
	E33	20	21.7±3.0	1.7±0.3	1.53±0.19	30±1
DL75+P3HB	E21	5	28.4±3.7	2.2±0.5	1.84±0.18	30±1
	E22	10	24.8±1.7	1.6±0.2	2.01±0.11	29±2
	E23	20	21.7±3.9	1.7±0.3	1.59±0.15	31±2
DL50+P3HB	E11	5	24.8±3.7	1.7±0.5	1.85±0.18	26±3
	E12	10	26.2±4.5	2.4±0.7	1.61±0.19	29±2
	E13	20	21.0±2.4	3.5±1.0	1.32±0.09	32±3

[a]Preparation method depicted in Scheme 1. [b]SR50: SR prepared using 50% methanol in water. DL50: DL prepared using 50% methanol in water. DL75: DL prepared using 75% methanol in water. DL100: DL prepared using 100% methanol.

films were not significantly different compared to that of P3HB films. Young's moduli of OL-P3HB films were not significantly different from those of P3HB films. SR-added P3HB films exhibited lower Young's moduli compared to P3HB films. Young's moduli of DL-added P3HB films were lower than those of P3HB films, but higher than those of SR-P3HB films. These observations indicate that SR-added films exhibited more adjusted mechanical properties (higher elongations at break and lower Young's moduli) compared to OL- and DL-added films.

4. Molecular Weights and Chemical Properties of Lignin and its Derivatives on the Mechanical Properties of Films

The adjusted mechanical properties of P3HB-based films were investigated using two variables of molecular weight and chemical property of lignin-derived additives (OL, SR, and DL in this study). The addition of high-molecular-weight lignin derivatives can adjust the crystalline structure of P3HB films. Notably, the size of lignin derivatives added to P3HB films increased with increasing molecular weight. In addition, the chemical properties of lignin-derivatives can determine the interaction between P3HB and additives for adjusting the mechanical properties of blended films.

First, the molecular weights of lignin-derivatives were measured using GPC (Fig. 4 and Table 5). The GPC measurements indicate that the molecular weights decreased in the order of OL>SR100>SR75>SR50≥DL100>DL75>DL50: OL exhibited M_w=2,970±297 g/mol and M_n=846±123 g/mol achieving PDI=3.5 while DL50 exhibited the lowest M_w=532±45 g/mol and M_n=307±12 g/mol with PDI=1.7. The PDIs of DL and SR were also smaller than those of OL, indicating a more uniform distribution of molecular weight.

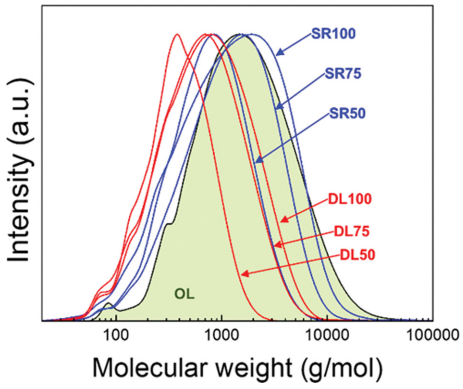

Fig. 4. GPC results of OL and its derivatives.

DL and SR exhibited lower molecular weights while OL exhibited M_w=2,970±297 g/mol and M_n=846±123 g/mol achieving PDI=3.5. For both SR (entries D1-D3) and DL (entries E1-E3), the molecular weights (M_ws) decreased with increasing methanol concentra-

Table 5. Molecular weights of OL and its derivatives measured using GPC

Entry	Lignin or lignin derivative	M_w (g/mol)	M_n (g/mol)	PDI
A, B, C	OL	2,970±297	846±123	3.5
D3	SR100	2,401±275	609±2	3.9
D2	SR75	1,886±120	679±16	2.8
D1	SR50	1,055±5	519±1	2.0
E3	DL100	1,077±68	422±20	2.6
E2	DL75	907±78	413±6	2.2
E1	DL50	532±45	307±12	1.7

Table 6. Quantities of hydroxyl groups in the lignin or its derivatives measured using ^{31}P-NMR

Sample	Carboxylic OH (mmol/g)	Phenolic OH (mmol/g)				Aliphatic OH (mmol/g)	Total OH (mmol/g)
		p-Coumaryl	Guaiacyl	Syringyl	Sum of phenolic OH		
OL	0.03	0.07	0.66	1.14	2.07	1.06	3.15
SR100	0.03	0.23	1.22	1.54	3.33	0.10	3.45
SR75	0.06	0.20	0.91	1.20	2.57	0.20	2.82
SR50	0.06	0.20	0.97	1.33	2.74	0.18	2.98
DL100	0.05	0.27	1.53	1.90	3.99	0.32	4.36
DL75	0.08	0.32	1.26	1.62	3.38	0.54	4.00
DL50	0.05	0.31	1.27	1.68	3.46	0.62	4.13

tion in the order of OL>SR100>SR75>SR50≥DL100>DL75>DL50. DL50 exhibited the lowest M_w=532±45 g/mol and M_n=307±12 g/mol with PDI=1.7. The PDIs of DL (1.7-2.6) and SR (2.0-3.9) were also smaller than those of OL (3.5), except for SR100, indicating a more uniform distribution of molecular weight.

Based on the molecular weight of lignin derivatives, the mechanical properties of films were investigated. Compared to the P3HB film (entry C0), the addition of OL, SR, and DL did not significantly modify the tensile strength, although the highest tensile strength was observed for the 5-10 wt% SR50-added P3HB film (33.0-33.2 MPa vs. 27.0 MPa for the P3HB film). These observations indicate that the molecular weight, or particle size, of lignin derivatives did not significantly adjust the tensile strength of films. The elongation at break was higher for SR- and DL-added films compared to P3HB films; however, the OL-added films did not exhibit increased elongation at break. Young's modulus was significantly lower for SR-added films compared to DL-added films. SR100- and SR75-added films exhibited 1.02-1.17 GPa and 0.98-1.17 GPa, respectively, lower than DL-added films. Notably, SR50-added films exhibited 1.60-1.72 GPa Young's moduli, higher than those of SR100- and SR50-added films.

The effects of molecular weights of lignin derivatives on the mechanical properties of films can be summarized as follows (Figs. 2, 3 and Tables 3, 4): (i) the molecular weights of lignin derivatives did not significantly adjust the tensile strength of films; (ii) the highest elongations at break and lowest Young's modulus were observed for the intermediate molecular weights of SR-added P3HB films. Given that the mechanical properties were not completely determined by the molecular weight of lignin derivatives, the effects of chemical properties, i.e., hydroxyls on lignin derivatives measured using ^{31}P NMR of phosphorous-treated lignin (Table 6) [23], were investigated. SR exhibited lower quantities of OH (2.82-3.45 mmol/g) compared to those of OL (3.15 mmol/g) and DL (4.00-4.36 mmol/g). For both SR and DL, the largest quantities of phenolic OH were observed when 100% methanol solvent was used for the lignin depolymerization process.

During the depolymerization of OL to phenolic monomers, SR, and DL, phenolic monomers and DL were fully dissolved in the solvent after the reaction, while SR was precipitated as depicted in Scheme 1 and described in the section on materials and method. These observations indicate that SR is hydrophobic to be precipitated in methanol or aqueous methanol solution, and DL is hydrophilic to be dissolved in these solutions. Given that P3HB is highly hydrophobic to be dissolved in chloroform, but insoluble in water or methanol, the hydrophobic SR must strongly interact with hydrophobic P3HB. Uniformly well-dispersed SR particles can more easily suppress the continuity of crystalline P3HB film, reducing the film's stiffness for decreasing Young's modulus [5]. The increased elongation at break of SR-added P3HB films can also be attributed to less stiffness of films.

5. Morphology of Films Measured Using SEM

The SEM images of P3HB-OL films displayed a similar morphology depending on the type and concentration of lignin derivatives in P3HB (Figs. 5 and 6). Adjusting their mechanical properties by morphology was not clear. The surface of films exhibited pores formed by the fiber-like structure (Fig. 5). The cross-sections of films also exhibited dense structures (Fig. 6).

6. Optical Properties of Films Using UV-Vis

The optical properties of P3HB-OL films were observed using UV-Vis (Fig. 7, 8, and Table 7); the UV protection abilities of the films were confirmed. The visible-transmitting but UV-protecting films were prepared by adding UV-absorbing lignin to transpar-

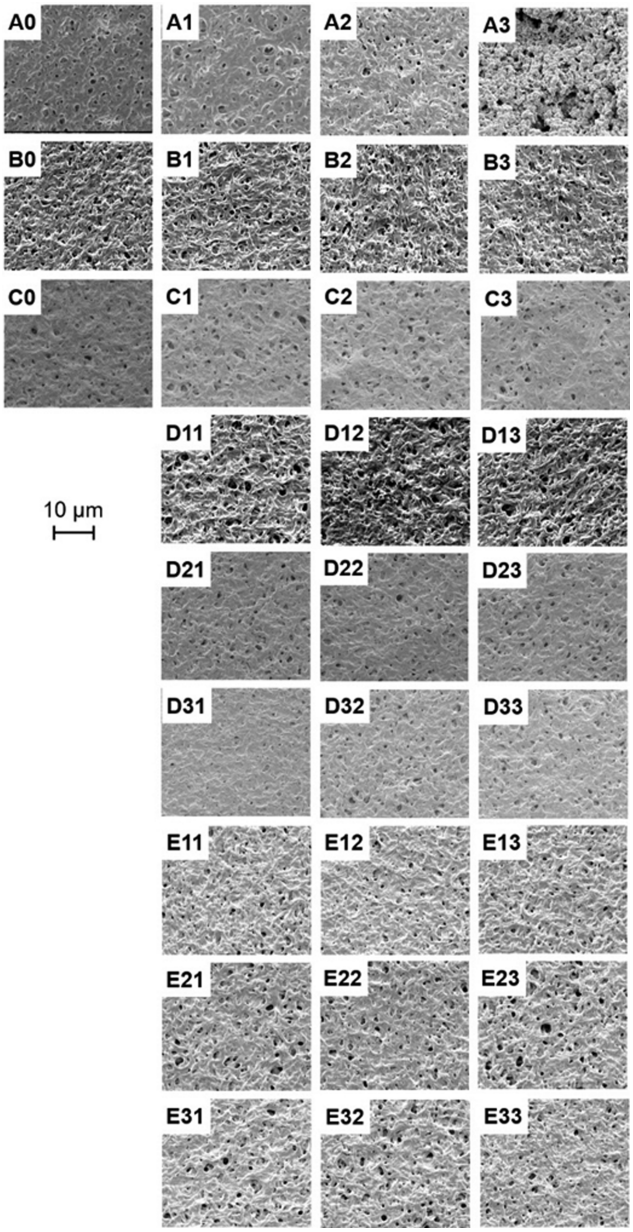

Fig. 5. Top view of SEM images of films containing P3HB and lignin derivatives.

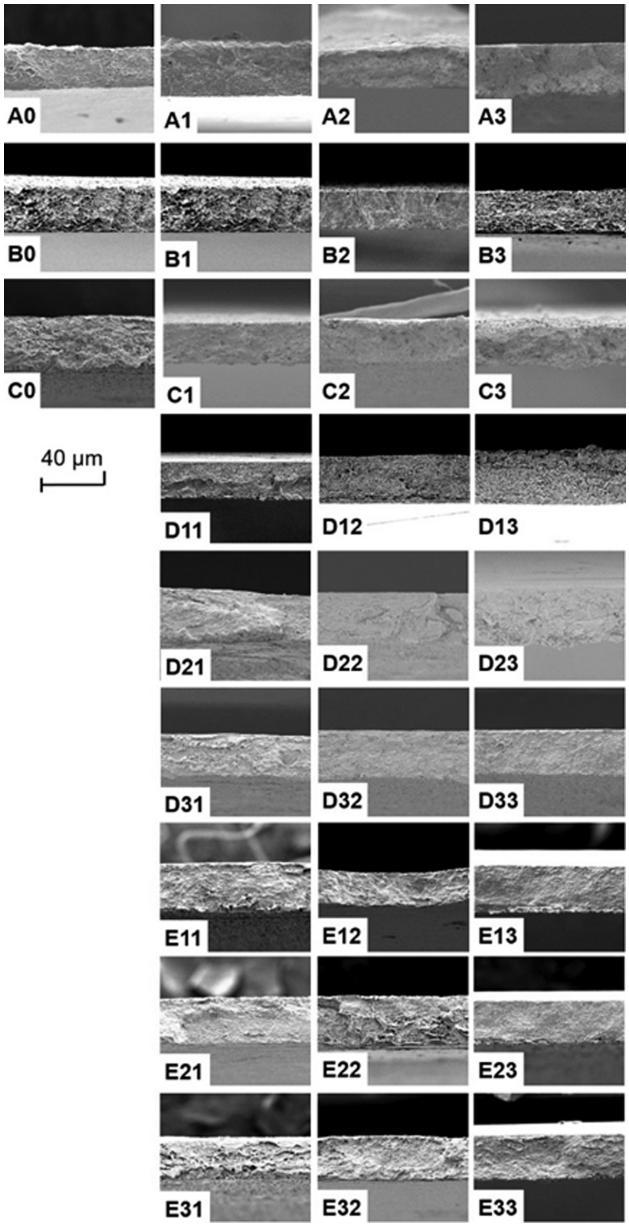

Fig. 6. Cross-sectional view of SEM images of films containing P3HB and lignin derivatives.

ent P3HB films. Because of the lignin-composing phenolic units absorbing UV, almost no transmission at 300 nm was observed on the OL-containing films except for entry E11, while the P3HB film without adding OL exhibited a transmittance higher than 80% at 300-800 nm. The transmittance decreased as the content of lignin derivatives increased from 0 to 20%. Because of the significant absorption of UVA and UVB for almost all P3HB-OL films except entry E11, a higher transmittance in the visible range may indicate a more transparent film with improved UV protection. The UV absorbing and visible transmitting abilities of films were compared (Table 7, Fig. 7, and Fig. 8). The addition of OL to P3HB significantly improved the UV protection (entries A0-3, B0-3, and C0-3 in Table 7, Figs. 7, and 8). For the film preparation method (entries Cs) selected in this study, 87.9% visible transmittance of visible light decreased to 61.6, 43.6, and 24.8% by adding 5, 10, 20% OL, respectively (entries C1-3). Compared to P3HB-OL films, higher visible transmittances of 41.8-78.3 (entry E11-13, adding DL50), 37.5-73.0 (entry E21-23, adding DL75), and 33.7-68.4% (entry E31-33, adding DL100) were observed by adding DL. By adding SR, higher visible transmittances of 23.2-51.2 (entries D11-13, adding SR50), 21.7-49.7 (entries D21-23, adding SR75), and 25.9-57.6% (entries D31-33, adding SR100) were not significantly different from those of P3HB-OL films. The improved visible transmittance with complete UV protection for P3HB-DL films can be attributed to the improved dispersion of smaller lignin derivatives obtained by the formation of DL with a smaller molecular weight. Understanding visibly transparent but almost completely UV-protecting P3HB-DL films requires further characterization of films that we are cur-

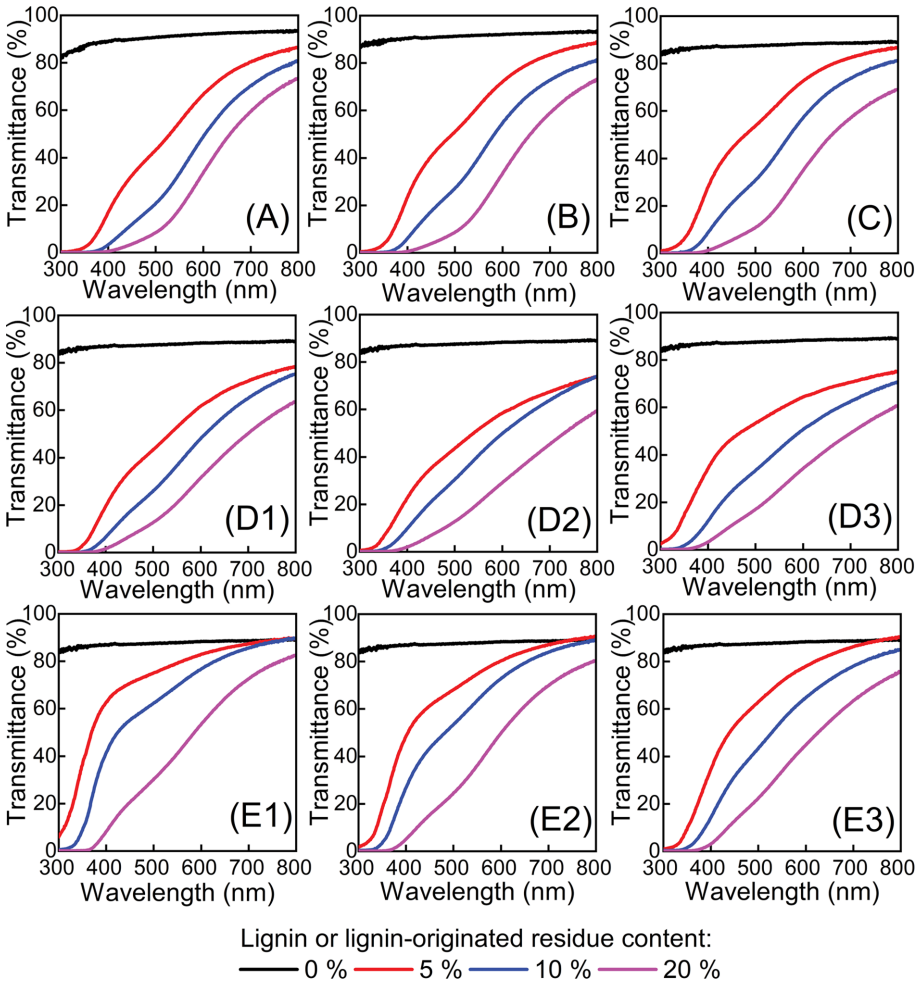

Fig. 7. UV-Vis results of films containing P3HB and lignin derivatives depending on lignin content.

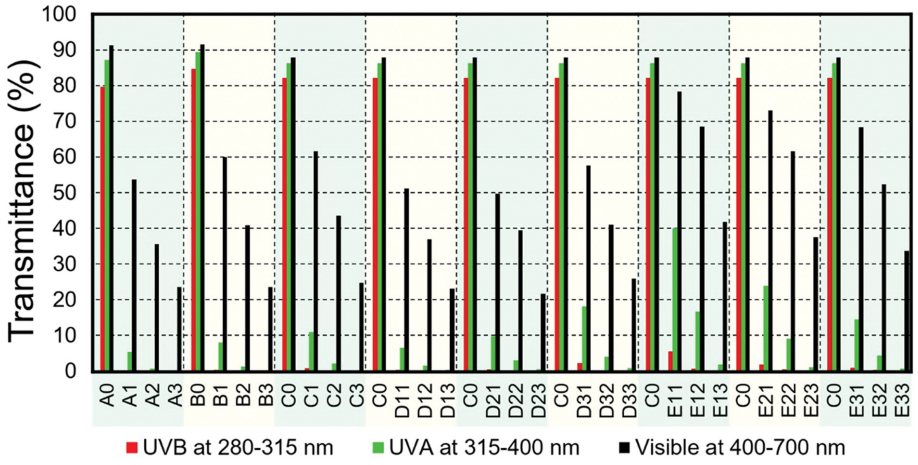

Fig. 8. Optical properties of films containing P3HB and lignin derivatives.

rently investigating.

CONCLUSIONS

We manipulated the mechanical and optical properties of P3HB film by adding OL. The adjusted properties can be attributed to the interaction between P3HB and lignin derivatives. When chemically modified depolymerized products, SR and DL in this study, were added to P3HB for preparing blended films, a decreased Young's modulus for blended films and increased UV protection

Table 7. Optical properties of films containing P3HB and lignin derivatives

Film	Entry	Lignin derivative content (%)	Transmittance of UVB at 280-315 nm (%)	Transmittance of UVA at 315-400 nm (%)	Transmittance of visible at 400-700 nm (%)	Transmittance at 800 nm (%)	UPF	UPF rating
P3HB film (sonicating P3HB at room temperature, then stirring at room temperature)	A0	0	81.6	87.2	91.3	93	1	-
	A1	5	0.3	5.5	53.7	86	146	50+
	A2	10	0.1	0.7	35.6	80	1,079	50+
	A3	20	0.0	0.1	23.6	73	2,210	50+
P3HB film (sonicating P3HB at room temperature, then stirring at 80 °C)	B0	0	86.4	89.4	91.6	93	1	-
	B1	5	0.5	8.2	60.0	89	91	50+
	B2	10	0.1	1.4	40.9	81	676	50+
	B3	20	0.0	0.1	23.6	73	2,068	50+
P3HB film (stirring at 80 °C)	C0	0	83.7	86.2	87.9	89	1	-
	C1	5	1.0	11.1	61.6	87	51	50+
	C2	10	0.1	2.3	43.6	81	418	50+
	C3	20	0.0	0.3	24.8	69	1,815	50+
SR50+P3HB	D11	5	0.3	6.7	51.2	78	135	50+
	D12	10	0.1	1.7	36.9	75	481	50+
	D13	20	0.1	0.4	23.2	63	1,189	50+
SR75+P3HB	D21	5	0.6	9.8	49.7	74	69	50+
	D22	10	0.2	3.1	39.5	74	288	50+
	D23	20	0.1	0.5	21.7	60	1,144	50+
SR100+P3HB	D31	5	2.8	18.1	57.6	75	21	20
	D32	10	0.2	4.1	41.1	71	209	50+
	D33	20	0.1	0.9	25.9	61	843	50+
DL50+P3HB	E11	5	6.8	39.8	78.3	90	9	-
	E12	10	0.7	16.9	68.5	90	51	50+
	E13	20	0.1	1.9	41.8	82	451	50+
DL75+P3HB	E21	5	2.1	24.0	73.0	91	23	20
	E22	10	0.4	9.2	61.6	89	98	50+
	E23	20	0.1	1.2	37.5	80	560	50+
DL100+P3HB	E31	5	1.1	14.7	68.4	91	44	40
	E32	10	0.4	4.4	52.4	85	162	50+
	E33	20	0.2	0.7	33.7	76	553	50+

were achieved depending on the added lignin derivatives. While the P3HB films exhibited a low elongation at break (≤2.0%), the addition of SR and DL increased the elongation at break (up to 4.9%). SR-added films also exhibited lower Young's modulus (0.98± 0.11 GPa), that is, 50% of the Young's modulus of P3HB films. The hydrophobicity improved the dispersion of SR in P3HB films, which adjusted the mechanical properties of blended films by suppressing the continuity of crystalline P3HB films. Compared to the P3HB films, the addition of lignin derivatives blocked UV, but allowed the visible light to pass through, particularly for P3HB-DL films. Based on these observations, the improved optical and mechanical properties were manipulated by preparing P3HB-based films blended with lignin derivatives. Given that the byproducts, i.e., DL and SR, prepared during the production of phenolic monomers from lignin were used for the preparation of sustainable biodegradable films, this study can contribute to the economic feasibility of lignin valorization.

ACKNOWLEDGEMENTS

This work was supported by the Korea Institute of Science and Technology (KIST) Institutional Program (2E31853).

CONFLICTS OF INTEREST

There are no conflicts to declare.

SUPPORTING INFORMATION

Additional information as noted in the text. This information is

available via the Internet at http://www.springer.com/chemistry/journal/11814.

REFERENCES

1. Z. A. Raza, S. Abid and I. M. Banat, *Int. Biodeterior. Biodegrad.*, **126**, 45 (2018).
2. S. Qian, X. Dai, Y. Qi and H. Ren, *BioResources*, **10**, 3169 (2015).
3. Y.-W. Wang, Q. Wu and G.-Q. Chen, *Biomaterials*, **24**, 4621 (2003).
4. P. Anbukarasu, D. Sauvageau and A. Elias, *Sci. Rep.*, **5**, 17884 (2015).
5. I. Lugoloobi, X. L. Li, Y. Zhang, Z. Mao, B, Wang, X. Sui and X. Feng, *Int. J. Biol. Macromol.*, **165**, 3078 (2020).
6. P. Vostrejs, D. Adamcová, M. D. Vaverková, V. Enev, M. Kalina, M. Machovsky, M. Šourková, I. Marova and A. Kovalcik, *Rsc Adv.*, **10**, 29202 (2020).
7. Q. Xing, D. Ruch, P. Dubois, L. Wu and W.-J. Wang, *ACS Sustain. Chem. Eng.*, **5**, 10342 (2017).
8. L. R. Chiappero, S. S. Bartolomei, D. A. Estenoz, E. A. B. Moura and V. V. Nicolau, *J. Polym. Environ.*, **29**, 450 (2020).
9. A. Gregorova, S. Redik, V. Sedlarik and F. Stelzer, *Lignin-containing polyethylene films with antibacterial activity*, NANOCON International Conference, TANGER Ltd., Ostrava, Brno, Czech Republic, 184 (2011).
10. J. Yang, Y. C. Ching and C. H. Chuah, *Polymers*, **11**, 751 (2019).
11. Y. Kim, J. Suhr, H.-W. Seo, H. Sun, S. Kim, I.-K. Park, S.-H. Kim, Y. Lee, K.-J. Kim and J.-D. Nam, *Sci. Rep.*, **7**, 43596 (2017).
12. B. Rukmanikrishnan, S. Ramalingam, S. K. Rajasekharan, J. Lee and J. Lee, *Int. J. Biol. Macromol.*, **153**, 55 (2020).
13. H. Sadeghifar and A. Ragauskas, *Polymers*, **12**, 1134 (2020).
14. M. Paulsson and J. Parkås, *BioResources*, **7**, 5995 (2012).
15. S. Oh, S. Gu, J.-W. Choi, D. J. Suh, H. Lee, C. S. Kim, K. H. Kim, C.-J. Yoo, J. Choi and J.-M. Ha, *J. Environ. Chem. Eng.*, **10**, 108085 (2022).
16. A. Karnitski, J.-W. Choi, D. J. Suh, C.-J. Yoo, H. Lee, K. H. Kim, C. S. Kim, K. Kim and J.-M. Ha, *Catal. Today*, **411-412**, 113844 (2022).
17. S. Gu, J.-W. Choi, H. Lee, D. J. Suh, J. Choi and J.-M. Ha, *Environ. Pollut.*, **268**, 115674 (2021).
18. J. B. Sluiter, R. O. Ruiz, C. J. Scarlata, A. D. Sluiter and D. W. Templeton, *J. Agric. Food Chem.*, **58**, 9043 (2010).
19. D. W. Templeton, C. J. Scarlata, J. B. Sluiter and E. J. Wolfrum, *J. Agric. Food Chem.*, **58**, 9054 (2010).
20. M. Kim, D. Son, J.-W. Choi, J. Jae, D. J. Suh, J.-M. Ha and K.-Y. Lee, *Chem. Eng. J.*, **309**, 187 (2017).
21. D. Son, S. Gu, J.-W. Choi, D. J. Suh, J. Jae, J. Choi and J.-M. Ha, *J. Ind. Eng. Chem.*, **69**, 304 (2019).
22. A. Granata and D. S. Argyropoulos, *J. Agric. Food Chem.*, **43**, 1538 (1995).
23. Y. Pu, S. Cao and A. J. Ragauskas, *Energy Environ. Sci.*, **4**, 3154 (2011).
24. H. Ben and J. R. Ferrell III, *RSC Adv.*, **6**, 17567 (2016).
25. Y. Lu, Y.-C. Lu, H.-Q. Hu, F.-J. Xie, X.-Y. Wei and X. Fan, *J. Spectrosc.*, **2017**, 1 (2017).
26. X. Meng, C. Crestini, H. Ben, N. Hao, Y. Pu, A. J. Ragauskas and D. S. Argyropoulos, *Nat. Protoc.*, **14**, 2627 (2019).
27. R. V. Chernozem, O. Guselnikova, M. A. Surmeneva, P. S. Postnikov, A. A. Abalymov, B. V. Parakhonskiy, N. De Roo, D. Depla, A. G. Skirtach and R. A. Surmenev, *Appl. Mater. Today*, **20**, 100758 (2020).
28. S. Phongtamrug and K. Tashiro, *Macromolecules*, **52**, 2995 (2019).

Supporting Information

Visibly transparent UV protection and adjusted mechanical properties of films composed of lignin-derived wastes and poly[(R)-3-hydroxybutyric acid]

Aliaksandr Karnitski[*,], Jae-Wook Choi[*], Heesuk Kim[**,***], Chun-Jae Yoo[*], Hyunjoo Lee[*,**], Dong Jin Suh[*], Kwang Ho Kim[*,**], Changsoo Kim[*,**], Kyeongsu Kim[*,**], and Jeong-Myeong Ha[*,**,†]**

*Clean Energy Research Center, Korea Institute of Science and Technology, Seoul 02792, Korea
**Division of Energy and Environment Technology, KIST School, Korea University of Science and Technology, Seoul 02792, Korea
***Soft Hybrid Materials Research Center, Korea Institute of Science and Technology, Seoul 02792, Korea
(*Received 11 November 2022* • *Revised 3 January 2023* • *Accepted 31 January 2023*)

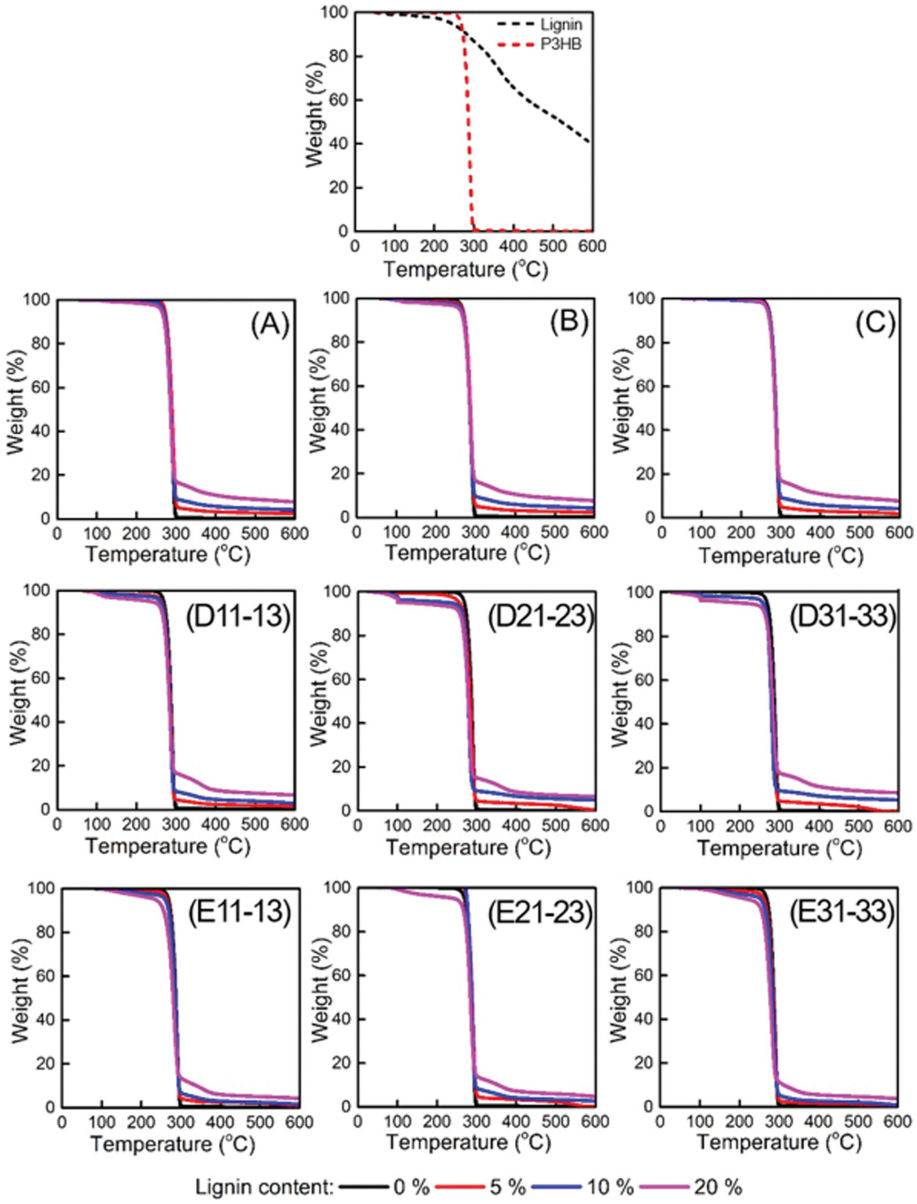

Fig. S1. Thermogravimetry results of lignin, P3HB, and mixtures of entries (A, B, C, D1-3, and E1-3).

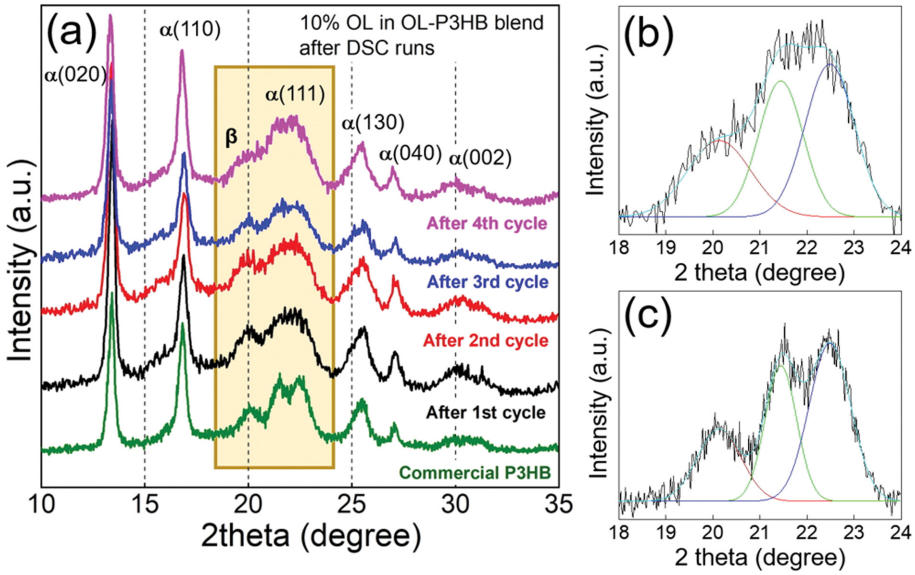

Fig. S2. (a) XRD results of a mixture of 10% OL and 90% P3HB after DSC measurements. Detailed XRD results (b) after the fourth DSC cycle and (c) commercial P3HB at 2θ=18-24°.

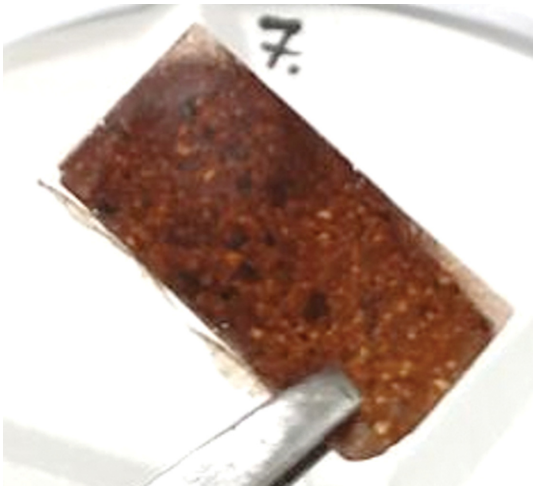

Fig. S3. Films prepared by hot pressing of PHB and OL (10% OL at 175 °C for 15 min pressed at 5,000 psig).